

# Synthesis, investigation and practical application in lithium batteries of some compounds based on vanadium oxides

E. Shembel <sup>a</sup>, R. Apostolova <sup>a</sup>, V. Nagirny <sup>a</sup>, D. Aurbach <sup>b,\*</sup>, B. Markovsky <sup>b</sup>

<sup>a</sup> Ukrainian State Chemical Technology University, 320005 Dnepropetrovsk, Ukraine

<sup>b</sup> Department of Chemistry, Bar-Ilan University, 52900 Ramat-Gan, Israel

Received 28 January 1999; accepted 31 January 1999

## Abstract

In this paper, we investigate the inter-relationship between the conditions of the electrochemical synthesis of vanadium oxide compounds, their structural and morphological characteristics, kinetic parameters of the redox processes, and charge–discharge performance of lithium batteries with vanadium oxide cathodes. The materials studied were  $V_2O_{5-y}$  oxides and those with inserted sodium ions (Na–vanadium oxide compounds, Na–VOC) obtained electrochemically in the form of compact deposits on a metal substrate. The electrochemical synthesis of the oxides has been performed from aqueous vanadyl sulphate solutions. Optimal synthesis conditions (current density, pH, temperature, vanadyl sulphate and sodium sulphate concentrations), and subsequent optimal thermal treatment of the oxides, which provide high electrochemical activity of the cathode material and good adhesion of the oxide to the metal substrate, have been elucidated. A correlation between the structure of the vanadium oxides and Na–VOC, their morphology, impedance characteristics of the cathode, and lithium-ion solid state diffusion in the host cathode bulk has been established and discussed. A combination of analytical techniques (XRD, IR spectroscopy, TGA, BET, SEM) and electrochemical methods (cyclic voltammetry, chronopotentiometry, GITT, EIS) has been used in this study. © 1999 Elsevier Science S.A. All rights reserved.

**Keywords:** Lithium rechargeable batteries; Vanadium oxides; Structural and morphological characteristics: electrode reactions/non-aqueous; Diffusion coefficients

## 1. Introduction

Cathodes based on vanadium oxides are very promising candidates for rechargeable lithium batteries due to their high specific charge capacity [1]. Indeed, since 1970, a large amount of publications on  $Li_xVO_y$  materials and their application in lithium batteries has appeared in the literature. The reversible lithium intercalation in vanadium pentoxide was first studied by Whittingham [2]. Much attention has been paid in recent years to the preparation of cathodes based on  $V_2O_5$ , and  $M_xV_2O_5$  bronzes (where  $M = Na^+, K^+, Mn^{2+}$ ),  $KV_6O_{13}$ , their structure and electrochemical performance in lithium power sources and in electrochromic devices. When examining recent literature, we see that  $V_2O_5$  is still considered to be one of the most promising cathodes for lithium batteries [3].

One of the main problems in the use of  $V_2O_5$  and  $M_xV_2O_5$  cathodes for rechargeable lithium batteries is their capacity fading during prolonged charge–discharge cy-

cling. This can probably be attributed to irreversible changes in the oxide structure occurring upon cycling. It appears that the stability and the capacity of these cathodes are considerably dependent upon the conditions of the vanadium oxide and bronzes synthesis. Special attention was focused on chemical [4–9] methods of preparation of these materials, physical methods of obtaining thin layers [10,11], and the electrochemical methods of synthesis of  $V_2O_5$  and  $M_xV_2O_5$  from aqueous solutions [12–22], aprotic electrolytes [23] and molten salts [24]. By using electrochemical methods, one can easily vary synthesis conditions, and obtain compact and thin oxide deposits without any electroconductive additive or binder [14,21,22,25,26]. This fact is of special importance from the point of view of: (i) studying the mechanisms of the electrochemical processes, which are uncomplicated by macrokinetics that appear in composite electrodes with conducting additive and a binder, (ii) increasing specific discharge characteristics of cathodes in real batteries.

Modification of the  $V_2O_5$  structure by the introduction of different metal ions was suggested by a number of research groups who studied the correlation between the

\* Corresponding author. Tel.: +972-3-531-8317; Fax: +972-3-535-1250; E-mail: aurbach@ashur.cc.biu.ac.il

synthesis and the electrochemical properties of these materials. In Ref. [27], the authors drew attention to the fact that heterogeneous oxide vanadium compounds (oxide-vanadium bronzes) with inserted metal ions, possess some advantages (compared with ‘pure’  $V_2O_5$ ) as cathode materials for lithium secondary batteries. Examples of such advantages are: (i) lesser solubility of  $M_xV_2O_5$  in aprotic electrolyte solutions during cycling [20]; (ii) higher discharge capacities of vanadium oxide-iron and aluminum bronzes [28]; (iii) better adhesion of  $NaV_2O_5$  to metal substrates [29].

The electrochemical method of synthesis of  $V_2O_5$  and oxide vanadium bronze is complicated by the fact that vanadium exists in different oxidation states ( $V^{2+}$ ,  $V^{3+}$ ,  $V^{4+}$ ,  $V^{5+}$ ) in aqueous solutions [30]. Redox potentials of different ion-pairs of vanadium and their transformations are dependent on the pH value which, in turn, changes considerably during electrolysis. For instance, in Refs. [12,13], vanadium oxide was obtained on the cathode during electrolysis of metavanadate electrolyte solutions with  $K^+$  or  $Na^+$  ions as additives. However, the electrolytes were unstable, and the quality of deposits was poor. Andrukaitis et al. [17–22] also synthesized vanadium oxides from metavanadate electrolyte solutions comprising  $K^+$ ,  $Cs^+$ ,  $Rb^+$ ,  $Li^+$  or  $Na^+$  ions. The subsequent thermal treatment of the deposits led to a  $M_yV_6O_{13+\delta}$  cathode. The best results in galvanostatic cycling were obtained with a  $K_yV_6O_{13+\delta}$  cathode. Vanadium oxide compounds with inserted  $Na^+$  or  $Li^+$  ions could not be prepared by electrochemical deposition.

In our previous communication [29], the possibility of the electrochemical anodic synthesis of  $Na_{0.33}V_2O_5$  bronze from an aqueous solution of vanadyl sulphate was described. The adhesion of the deposit to the metal substrate was good, and cathodes prepared on the basis of this material showed reversible behaviour (lithium insertion–deinsertion processes) in aprotic lithium salt solutions. There are reports on the electrochemical behaviour of vanadium bronze of the  $K_xV_yO_z$  type synthesized by different methods, in lithium battery systems [21,22,31]. There are also reports on the behaviour of  $M_xV_2O_5$  ( $M = Ni, Mn, Co, Cu$ ) [32]. The formation features and electrochemical properties of  $M_xV_2O_5$  ( $M = Na^+, K^+, Cs^+, Ca^{2+}$ ) bronzes in melts of dimethylsulphone have been studied in Ref. [23]. Of special interest is the work of Bach et al. [33], devoted to the thermodynamic and kinetic investigation of lithium intercalation into  $V_2O_5$  and  $Na_{0.33}V_2O_5$  (the bronze was obtained by a sol–gel process). It was shown [33] that this bronze had some advantages over that obtained by a solid-state chemical reaction at 700°C. In addition, these authors described the influence of the lithium ion intercalation level on the lithium chemical diffusion coefficient, taking into account the distribution of vacancies in the bronze structure.

Comparison and analysis of the literature data clearly demonstrates that the method of synthesis of vanadium

bronzes has a strong influence both on their structure and on their electrochemical properties. In the present paper, we report on some properties of sodium–vanadium bronzes synthesized from an aqueous solution comprising vanadyl sulphate and sodium sulphate during the anodic oxidation of vanadium ( $V^{4+} \rightarrow V^{5+}$ ).

## 2. Experimental

We have shown in previous communications [26,29] that vanadium oxides can be deposited electrochemically (galvanostatically) onto stainless steel substrates using a vanadyl sulphate solution. After optimization of the solution’s composition and the parameters of the electrochemical synthesis, we could reach high stability of the electrolyte, as well as of the electrochemical synthesis process.

In the present work, we synthesized vanadium oxides with inserted sodium ions by using an electrolyte solution comprising vanadyl sulphate and sodium sulphate (1.25–25.0 g l<sup>-1</sup> of  $Na^+$ ). It should be stressed that the electrolyte stability is extremely important in this case. In addition, the electrolyte is very sensitive to changes of the electrolysis conditions because of the  $V^{4+} \rightarrow V^{3+}$  reduction process. Important factors are the amount of the background (non-reacting) electrolyte in the solution, the pH and the duration of the electrolysis. We have shown that the optimal conditions for obtaining vanadium oxides with inserted sodium ions are as follows: vanadyl sulphate concentration in the 0.1–0.35 M l<sup>-1</sup> range, current density of 7.5–12.5 mA cm<sup>-2</sup>, pH of 1.5–1.8 and temperature of 80–85°C. Compact  $Na-VO_x$  deposits could be obtained on stainless steel plates (SSP) or grids. Dispersed powders could also be deposited onto a SSP. The electrochemically synthesized vanadium oxides were thermally treated at 100–500°C for about 2–7 h, or stored at room temperature for about 50 h. In the latter case, the oxide samples were additionally dried in vacuum at room temperature.

A combination of analytical techniques (XRD, IR-spectroscopy, TGA, BET, SEM) and electrochemical methods (cyclic voltammetry, chronopotentiometry, GITT, EIS) were used in the present work. The application of these techniques, the electrochemical cells used, and the methods of cathode preparation procedures are described elsewhere [26].

## 3. Results and discussion

### 3.1. Structural and morphological investigation

Vanadium oxides prepared electrochemically from aqueous solutions comprising  $Na^+$  ions are characterized by better adhesion to the steel substrate than ‘pure’  $V_2O_5$  deposits obtained at the same electrolysis conditions from vanadyl sulphate solutions without  $Na_2SO_4$  [29]. Powders

of Na-VO<sub>x</sub> are more compact than those of V<sub>2</sub>O<sub>5</sub>. The powder of the Na-VO<sub>x</sub> consists of agglomerates (Fig. 1a)

comprised of small particles with an average diameter of about 10 μm (Fig. 1b). The specific surface area of the

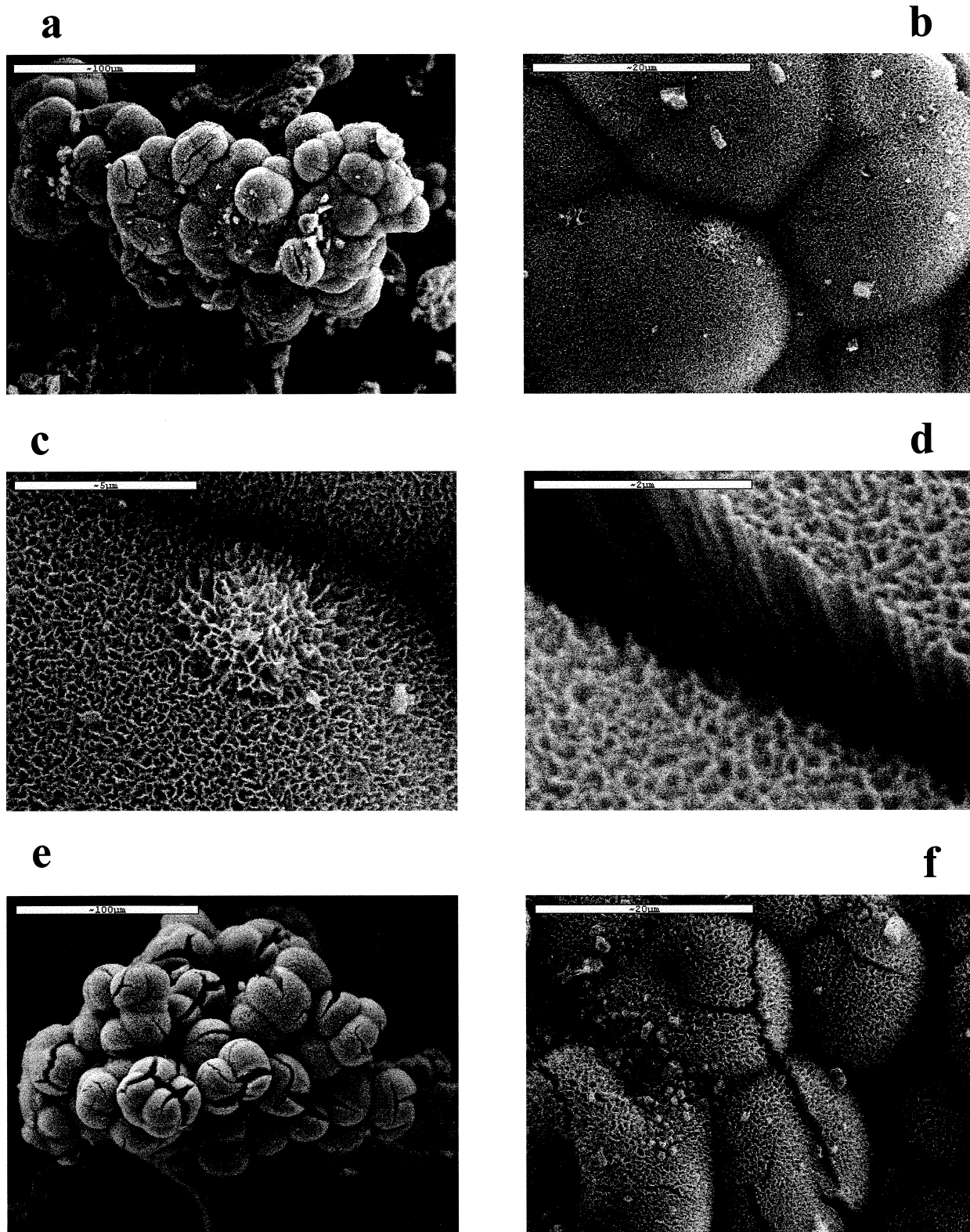


Fig. 1. SEM micrographs of the electrochemically synthesized Na-VO<sub>x</sub> (a,b,c,d,f) and 'pure' V<sub>2</sub>O<sub>5</sub> (e) a,b,c,d—samples stored after synthesis for about 48 h at room temperature; (d) a fracture of the Na-VO<sub>x</sub> particle; (e) the material was heated to 300°C for about 7.5 h; (f) the material was heated to 300°C, 2.5 h.

Na-VO<sub>x</sub> powder dried at room temperature for about 48 h was 1.44 m<sup>2</sup> g<sup>-1</sup> (as obtained by the BET method). The thermal treatment at  $t > 300^{\circ}\text{C}$  leads to microstress and cracking in the V<sub>2</sub>O<sub>5</sub> (Fig. 1e), as well as in the Na-VO<sub>x</sub> particles (f). Fig. 1d represents a fracture of an oxide particle, and clearly shows that it is continuous and non-porous.

According to the data obtained from TGA analysis of the Na-VO<sub>x</sub> samples, the maximal loss of mass upon heating occurs at temperatures up to 190°C due to liberation of water (about 1.09 mol per 1 mol of V<sub>2</sub>O<sub>5</sub>). Additional losses of strongly bound water may occur upon heating up to 420°C (up to 0.37 mol per 1 mol of V<sub>2</sub>O<sub>5</sub>). For vanadium oxide (V<sub>2</sub>O<sub>5</sub>), the amounts of ‘free’ and

bounded water were 0.84 and 0.16 mol per 1 mol of the oxide, respectively (as found by TGA analysis).

The XRD pattern of the Na-VO<sub>x</sub> sample stored at room temperature for about 52 h (Fig. 2, curve 1) exhibits sharp peaks, which are characteristic of highly dispersed crystalline materials. When comparing the XRD data obtained from V<sub>2</sub>O<sub>5</sub> (Fig. 2, curve 2) and Na-VO<sub>x</sub>, one can conclude that the introduction of sodium into the V<sub>2</sub>O<sub>5</sub>, thus forming the bronze, strongly influences the vanadium oxide structure: additional peaks emerge at  $\theta = 12.4^{\circ}$  ( $d = 3.59 \text{ \AA}$ ),  $\theta = 14.4^{\circ}$  ( $d = 3.1 \text{ \AA}$ ),  $\theta = 24.9^{\circ}$  ( $d = 2.998 \text{ \AA}$ ), and there is also a shift of the first line of the XRD pattern. The literature data regarding V<sub>2</sub>O<sub>5</sub> [4,34] and our studies of the electrochemically synthesized vanadium oxides

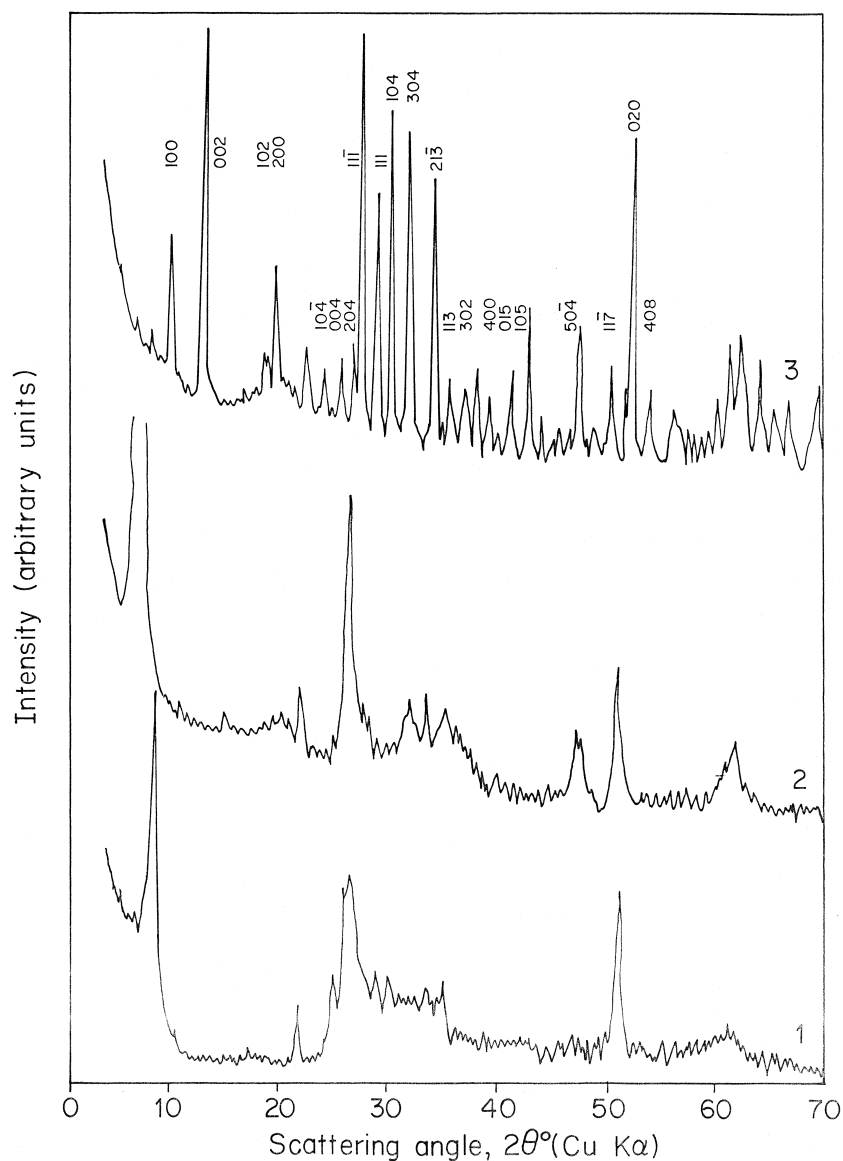


Fig. 2. XRD patterns of the electrochemically synthesized Na-VO<sub>x</sub> (curves 1 and 3) and ‘pure’ V<sub>2</sub>O<sub>5</sub> (curve 2): 1—the concentration of Na<sup>+</sup> in the synthesis electrolyte was 20 g l<sup>-1</sup>; the sample was stored after synthesis for about 52 h at room temperature; 2—the sample was stored for about 52 h at room temperature; 3—concentration of Na<sup>+</sup> in the synthesis electrolyte solution was 20 g l<sup>-1</sup>; the sample was heated after synthesis to 300°C for 7.5 h. The Miller indices are indicated.

[26,35] show that this XRD peak strongly depends on the water content in the oxide structure. As one can see from the results presented in this paper, the interplanar distance corresponding to this line decreases from  $d = 13.60 \text{ \AA}$  in the 'pure' vanadium pentoxide to  $d = 10.78 \text{ \AA}$  in  $\text{Na-VO}_x$ . In the latter compound, however, the water content is higher than in the 'pure'  $\text{V}_2\text{O}_5$ . Thus, we can conclude that the decreasing of the interplanar distance is connected to the oxide structural changes due to the sodium insertion, rather than to the reduction of the  $\text{H}_2\text{O}$  content. We assume that the formation of the  $\text{Na-VO}_x$  by the electrochemical process occurs via Na insertion into the  $\text{V}_2\text{O}_5$ , which is formed on the anode side. However, the mechanism of the Na insertion into the oxide crystalline structure requires special study and is beyond the scope of the present work. It will be presented in the next publication.

The subsequent thermal treatment of  $\text{Na-VO}_x$  samples in the range of  $300\text{--}500^\circ\text{C}$  leads to further changes in their structure (Fig. 2, curve 3), which correspond to the stoichiometry of  $\text{Na}_{0.33}\text{V}_2\text{O}_5$  and a monoclinic lattice of SG  $\text{C2/m}$ , comprising 6 formal units per one Bravais cell. The structure of the bronze obtained in our work corresponds to that of  $\text{Na}_{0.33}\text{V}_2\text{O}_5$  described in the literature [36]. The following are the parameters of the lattice:  $a = 10.078 \text{ \AA}$ ,  $b = 3.612 \text{ \AA}$ ,  $c = 15.435 \text{ \AA}$ ,  $\beta = 109.6^\circ$ . The formation of the  $\text{Na}_{0.33}\text{V}_2\text{O}_5$   $\beta$ -bronze occurs already at  $300^\circ\text{C}$ . Increasing the temperature up to  $500^\circ\text{C}$  stabilizes its structure, as evidenced by the contraction of the X-ray reflection band and the increase in the lines' intensity due to the heat treatment. Regarding IR-spectroscopic measurements of these compounds, peaks at  $1000 \text{ cm}^{-1}$ ,  $760 \text{ cm}^{-1}$  and  $540 \text{ cm}^{-1}$  characterize IR spectra obtained from both  $\text{V}_2\text{O}_5$  and  $\text{Na-VO}_x$ , heated to temperatures no higher than  $300^\circ\text{C}$ . Further thermal treatment up to  $550^\circ\text{C}$  leads to considerable changes in the  $\text{Na-VO}_x$  structure. The IR-spectrum of  $\text{Na-VO}_x$ , heated up to  $550^\circ\text{C}$  is very similar to that of the  $\beta$ -bronze  $\text{Na}_{0.33}\text{V}_2\text{O}_5$  [37]. The IR bands in the  $1000\text{--}400 \text{ cm}^{-1}$  range which correspond to the V–O bonds are strong, and change only slightly during the phase transitions which occur upon lithium-ion intercalation into the cathode. In contrast, the IR band in the  $500\text{--}200 \text{ cm}^{-1}$  range undergoes more pronounced changes upon the lithium-intercalation process. Our work in this area is currently in progress.

### 3.2. Electrochemical studies

Lithium intercalation and deintercalation processes were studied with thermally treated and untreated  $\text{Na-VO}_x$  cathodes. Fig. 3a shows the typical voltammetric behaviour of  $\text{Na-VO}_x$  cathodes stored at room temperature for about 48 h before measuring; a pair of cathodic and anodic peaks is observed in the cyclic voltammogram. As is seen from Fig. 3b, the lithium intercalation and deintercalation processes of the thermally treated sample differ considerably from those of the untreated electrodes. The voltammograms of

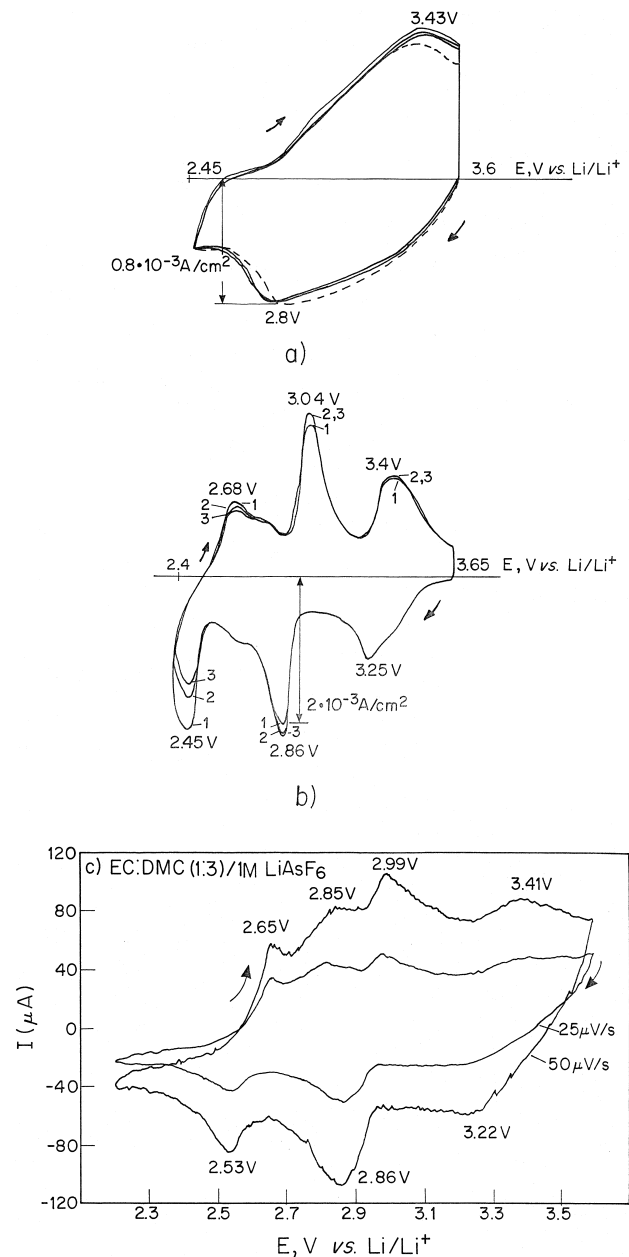


Fig. 3. (a) Cyclic voltammograms obtained at a scan rate of  $0.5 \text{ mV s}^{-1}$  in  $1 \text{ M LiClO}_4/\text{propylene carbonate (PC):dimethoxyethane (DME) (1:1)}$ , with  $\text{Na-VO}_x$  cathode, stored after electrochemical synthesis at room temperature for about 24 h and then in vacuum 6 h. Deposition electrolyte was  $\text{VOSO}_4\text{--}0.25 \text{ M l}^{-1}$ ,  $\text{Na}^+\text{--}20 \text{ g l}^{-1}$ . Successive cycles are shown. (b) Same as (a). Cathode of  $\text{Na-VO}_x$ , heated after electrochemical synthesis to  $300^\circ\text{C}$  for 7 h. Cycle numbers are indicated. (c) Same as (a) and (b). The scan rates were  $0.050$  and  $0.025 \text{ mV s}^{-1}$ . The electrolyte solution was  $1 \text{ M LiAsF}_6/\text{ethylene carbonate (EC):dimethyl carbonate (DMC) (1:3)}$ . The cathode ( $\text{Na-VO}_x$ ) was synthesized from an aqueous  $\text{VOSO}_4/\text{Na}_2\text{SO}_4$  solution. The  $\text{Na}^+$ -ion concentration was  $20 \text{ g l}^{-1}$ . The cathode material was treated at  $300^\circ\text{C}$  for 2.5 h after synthesis.

the heat treated  $\text{Na-VO}_x$  are characterized by three sets of relatively sharp anodic and cathodic peaks. We assume that this voltammetric behaviour indicates that the lithium insertion processes into  $\text{Na-VO}_x$  are accompanied by phase

transitions, as in the case of ‘pure’  $V_2O_5$ . It should be pointed out, however, that there are some differences in the influence of the thermal treatment on the electrochemical behaviour of ‘pure’  $V_2O_5$  and  $Na-VO_x$ . As has been already demonstrated in Ref. [26], thermal treatment of  $V_2O_5$  led to a shift in the cathodic and anodic peaks to higher potentials. When comparing the data of Fig. 3a and b, one can conclude that thermal treatment of the  $Na-VO_x$  leads to the emergence of anodic peaks in the more negative potential region. The first reduction peak in the cyclic voltammogram obtained with the cathode, based on the thermally treated  $Na-VO_x$ , appears at 3.25 V ( $Li/Li^+$ ), which is 0.3 V lower than the peak of the thermally treated  $V_2O_5$  (Fig. 3b). The peaks corresponding to the two subsequent reduction processes of the above cathode materials are located in approximately the same potential regions. Therefore, we assume that the biggest differences in the character of the phase transitions occur during lithium-ion intercalation/deintercalation, compared with cathodes based on ‘pure’  $V_2O_5$  and  $Na_{0.33}V_2O_5$  bronze, where they are in the first reduction stage.

The galvanostatic discharge curves measured with cathodes, based on  $Na-VO_x$  formed at room temperature with no further heat treatment, are smooth. Heat treatment of the  $Na-VO_x$  changes their discharge characteristics considerably. Plateaus located at potentials of 3.30 V, 2.90 V and 2.55 V appear, and can be attributed to phase transitions during lithium intercalation. Galvanostatic tests performed with  $Li/Na_{0.33}V_2O_5$  coin cells using 1 M  $LiClO_4$ /propylene carbonate-dimethoxyethane, 1:1 solutions have shown good cyclability of the electrochemically synthesized bronze  $Na_{0.33}V_2O_5$ . The discharge capacity during the first 10 cycles was about  $170 \text{ mA h g}^{-1}$  at

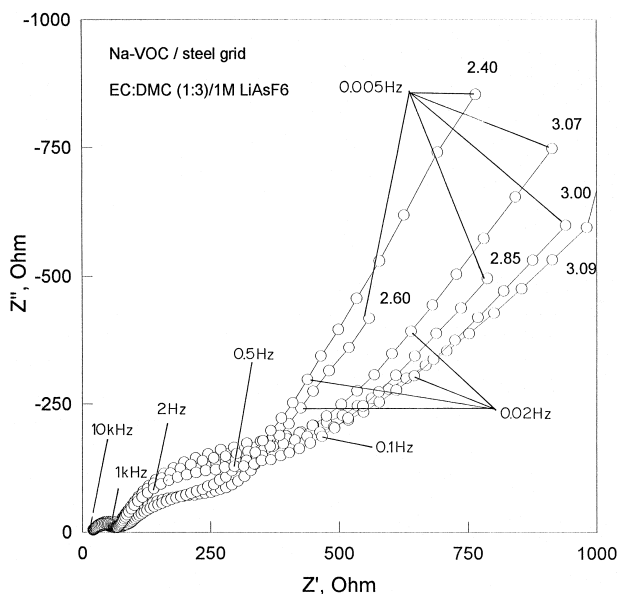


Fig. 4. A family of Nyquist plots measured with the  $Na-VO_x$  cathode related to Fig. 3c. The geometric area of the cathode was  $1.3 \text{ cm}^2$ . The potentials of the intercalation (V vs.  $Li/Li^+$ ) are shown on the curves.

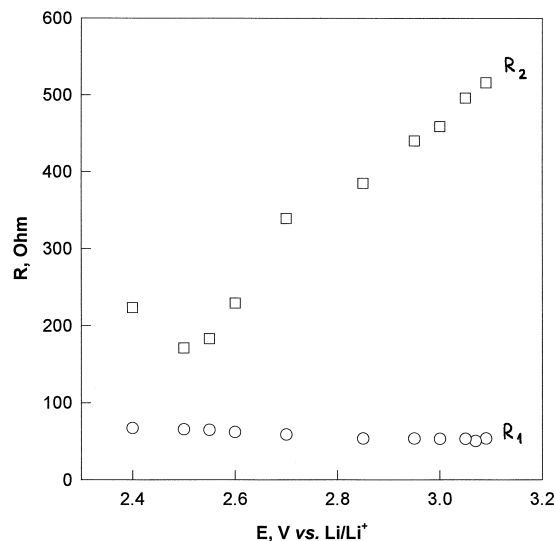


Fig. 5. Potential dependence of the  $R_1$  and  $R_2$  resistances corresponding to the 1st and 2nd semicircles in the Nyquist plots of Fig. 4 derived from these impedance spectra.

discharge and charge current values of  $200 \mu\text{A cm}^{-2}$  and  $100 \mu\text{A cm}^{-2}$ , respectively.

Fig. 3c shows cyclic voltammograms obtained at slow scan rates ( $50$  and  $25 \mu\text{V s}^{-1}$ ) with a cathode comprised of the heat treated ( $300^\circ\text{C}$ ,  $2.5 \text{ h}$ )  $Na-VO_x$  in an EC:DMC (1:3)/1 M  $LiAsF_6$  solution. Basically, the cyclic voltammograms of Fig. 3c are qualitatively similar to those of Fig. 3b in terms of the cathodic and anodic peak potential positions, although potentiodynamic responses have been obtained with different non-aqueous electrolyte solutions. A shoulder appearing between two anodic peaks at  $2.68 \text{ V}$  and  $3.04 \text{ V}$  in Fig. 3b corresponds probably to the  $2.85 \text{ V}$  peak in the voltammograms obtained at slow scan rates (Fig. 3c). A detailed study concerning the influence of the synthesis conditions, as well as the subsequent heat treatment of the cathode material and the nature of the non-aqueous electrolyte solutions and salts used, also on the electrochemical, morphological and structural characteristics of the  $Na$ -bronze cathodes during lithium intercalation/deintercalation is in progress, and will be reported on in the near future [35].

Typical complex plane impedance spectra of the  $Na-VO_x$  electrode (Fig. 4) consist of two depressed semicircles: one relates to the high frequency range ( $100 \text{ kHz}$ – $250 \text{ Hz}$ ), and the second to the medium–low frequency range ( $250 \text{ Hz}$ – $0.2 \text{ Hz}$ ). The  $R_1$  resistance related to the first semicircle changes only slightly with the potential of the intercalation (Fig. 5), and we assume that this semicircle in the Nyquist plots can be attributed to some kind of a surface layer, as proposed by Thomas et al. [38]. The existence of a surface layer adds to the electrode’s impedance resistance, which relates to  $Li^+$  ion migration through the film. In the case of the  $Na-VO_x$ , a surface layer can be formed on the cathode due to its interactions

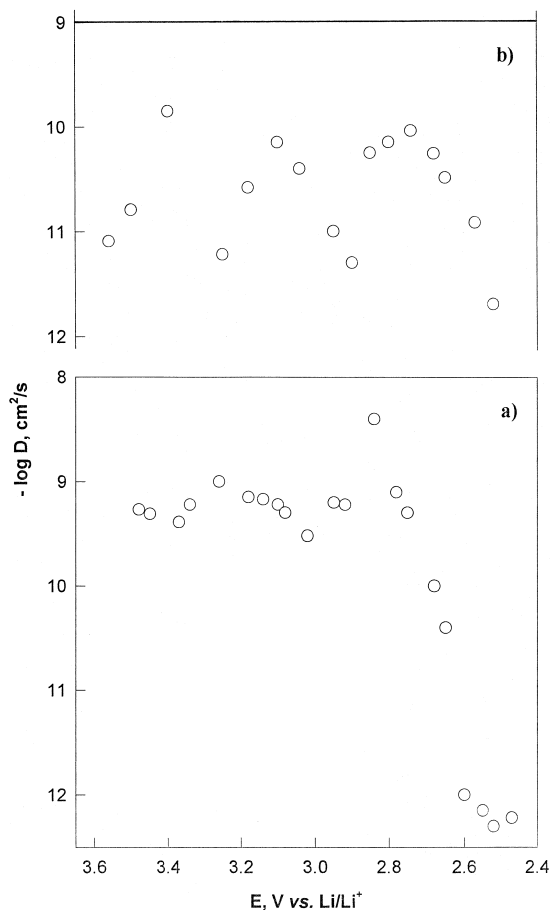


Fig. 6. (a) The dependence of the chemical diffusion coefficient (obtained by GITT [39]) of lithium ions on the potential during intercalation ( $\text{LiClO}_4/\text{PC:DME}$ ) of lithium into the cathode containing  $1.1 \text{ mg cm}^{-2}$  of  $\text{Na-VO}_x$  after storage at room temperature for about 24 h, and then in vacuum for 6 h. The concentration of the sodium ions in solution during synthesis was  $20 \text{ g l}^{-1}$ . (b) Same as (a). The  $\text{Na-VO}_x$  cathode, containing  $1.8 \text{ mg cm}^{-2}$ , was heated to  $300^\circ\text{C}$  for 5.5 h, after the electrochemical synthesis.

with solution species (e.g., oxidation of solvent molecules by  $\text{V}^{5+}$  ions, which are strong oxidizers). Regarding the  $R_2$  resistance that is strongly potential dependent, this can be attributed to the interfacial charge transfer. The inclined line in the low frequency range is associated with Warburg impedance of lithium ion solid-state diffusion in the cathode bulk. The chemical diffusion coefficient of  $\text{Li}^+$  ions calculated from the Warburg region varies in the range of  $3.0 \times 10^{-12}$  to  $6.5 \times 10^{-11} \text{ cm}^2 \text{ s}^{-1}$  during the entire intercalation reaction ( $3.09 \text{ V} \rightarrow 2.40 \text{ V vs. Li/Li}^+$ ).

Fig. 6a shows the dependence of the  $\text{Li}^+$  chemical diffusion coefficient (obtained by GITT [39]) on the potential of the intercalation process with  $\text{Na-VO}_x$ , which was not treated thermally after its electrochemical synthesis. The values of  $D$  change only slightly with potential in the range of  $3.50 \text{ V} - 2.80 \text{ V}$ , and they decrease considerably in the lower voltage region when the cathode is almost fully intercalated (Fig. 6a). It is interesting to note that thermal treatment ( $300^\circ\text{C}$ , 5.5 h) of this cathode material led to a

non-monotonous relationship of  $-\log D$  vs.  $E$  (Fig. 6b). The locations of the minima of the above  $-\log D$  vs.  $E$  curve correlate well with the peak potential positions of the corresponding voltammogram (Fig. 3b). A similar correlation was also discovered and discussed by Barker et al. [40] for  $\text{LiMn}_2\text{O}_4$  spinel cathodes, as well as in our recent studies of electrochemically synthesized  $\text{V}_2\text{O}_5$  cathode [26] and other transition metals oxides such as  $\text{LiMnO}_4$ ,  $\text{LiNiO}_2$ , and  $\text{LiCoO}_2$  in lithium battery systems [41,42]. We suggest that the non-monotonous behaviour with the potential of the chemical diffusion coefficient of  $\text{Li}^+$  ions can be explained in terms of attractive short-range interactions among the intercalation sites, and phase transitions in the host cathode material during lithium intercalation/deintercalation.

#### 4. Conclusions

(1) Electrochemical synthesis of sodium–vanadium oxide bronzes.  $\text{Na}_{0.33} \text{V}_2\text{O}_5$  from aqueous solutions comprising vanadyl sulphate and sodium sulphate has been successfully carried out. By this method,  $\text{Na-VO}_x$  compounds with reproducible structural and electrochemical characteristics could be obtained. These compounds insert lithium reversibly and show high cyclability.

(2) The inter-relationship between the conditions of the electrochemical synthesis and subsequent thermal treatment of the cathode materials ('pure'  $\text{V}_2\text{O}_5$  and  $\text{Na-VO}_x$ ), their structure, morphology and their electrochemical behaviour in lithium battery systems have been studied.

#### Acknowledgements

This work was supported by the Ukrainian and Israeli Ministries of Science within the framework of the joint Ukrainian–Israeli Binational Project for Exchange of Scientists (Project No. 2M/1420-97).

#### References

- [1] D.W. Murphy, P.A. Cristian, F.J. Disalvo, J.N. Caride, J. Electrochem. Soc. 126 (1970) 497.
- [2] M.S. Whittingham, J. Electrochem. Soc. 123 (1975) 315.
- [3] M. Winter, J.O. Besenhard, M.E. Spahr, P. Novak, Advanced Materials 10 (1998) 725.
- [4] S.-I. Pyun, J.-S. Bae, J. Power Sources 68 (1997) 669.
- [5] K. West, B. Zachau-Christiansen, S. Skaarup, Y. Saidi, J. Barker, I.I. Olsen, R. Pynenburg, R. Koksang, J. Electrochem. Soc. 143 (1996) 820.
- [6] M.G. Minnet, J.R. Owen, J. Power Sources 32 (1990) 81.
- [7] H.-K. Park, W.H. Smyrl, M.D. Ward, J. Electrochem. Soc. 142 (1995) 1068.
- [8] Y. Sato, T. Asada, H. Tokugawa, K. Kobayakawa, J. Power Sources 68 (1997) 674.
- [9] U. Von Sacken, J.R. Dahn, J. Power Sources 26 (1989) 461.

- [10] N. Kumagai, H. Kitamoto, M. Baba, S. Durand-Vidal, D. Devillieres, H. Groult, *J. Appl. Electrochem.* 28 (1998) 41.
- [11] K. West, B. Zachau-Christiansen, T. Jacobsen, *J. Power Sources* 43–44 (1993) 127.
- [12] A.S. Goncharenko, *Zh. Prikl. Khim.* 32 (1961) 151, in Russian.
- [13] A.S. Goncharenko, O.A. Suvorova, *Zh. Prikl. Khim.* 33 (1962) 846, in Russian.
- [14] V. Sato, T. Namura, H. Tanaka, K. Kobayakawa, *Electrochem. Soc. Lett.* 138 (1991) L37.
- [15] L.D. Burke, E.J.M. O'Sullivan, *J. Electroanal. Chem.* 11 (1980) 383.
- [16] Y. Sakurai, S. Okada, J. Yamaki, T. Okada, *J. Power Sources* 20 (1987) 173.
- [17] E. Andrukaitis, E.A. Bishenden, P.W.M. Jacobs, J.W. Lorimer, *J. Power Sources* 26 (1989) 475.
- [18] E. Andrukaitis, P.W.M. Jacobs, J.W. Lorimer, *Solid State Ionics* 27 (1988) 19.
- [19] E. Andrukaitis, P.W.M. Jacobs, J.W. Lorimer, *Solid State Ionics* 37 (1990) 157.
- [20] E. Andrukaitis, J.W. Lorimer, P.W.M. Jacobs, *Can. J. Chem.* 68 (1990) 1283.
- [21] E. Andrukaitis, *J. Power Sources* 43–44 (1993) 603.
- [22] E. Andrukaitis, *J. Power Sources* 54 (1995) 470.
- [23] J.P. Pereira-Ramos, R. Messina, J. Perichon, *J. Electroanal. Chem.* 218 (1987) 241.
- [24] E.V. Babenko, A.A. Fotiev, A.N. Baraboshkin, K.A. Kaliev, *J. Inorg. Chem.*, 23 (1978) 1241, 2253 (in Russian).
- [25] R.D. Apostolova, V.M. Nagirny, E.M. Shembel, 190th Meeting of the Electrochemical Society, San Antonio, Texas, Oct. 6–11, Meet. Abstr. PV-96-2. P. 178, The Electrochem. Society Proceedings Series, Pennington, NY, 1996.
- [26] E.M. Shembel, R.D. Apostolova, V.M. Nagirny, D. Aurbach, B. Markovsky, 9th International Li Battery Meeting, July 12–17, Edinburgh, Scotland, 1998.
- [27] J. Desilvestro, O. Haas, *J. Electrochem. Soc.* 137 (1990) .
- [28] P. Willman, J.P. Pereira-Ramos, R. Baddour-Hadjean, PCT/FR 92/01167.
- [29] E.M. Shembel, R.D. Apostolova, V.M. Nagirny, The 194th Meeting of the Electrochem. Soc., Boston, 1–6 November, Extended Abstracts V. 98-2, abstr. N 172, Pennington, NJ, USA, 1998.
- [30] E. Deltombe, N. Zoubov, M. Porbaix, *Atlas of Electrochem. Equilibria in Aqueous Solutions*, Pergamon, London, 1966, p. 234.
- [31] V. Manev, A. Momchilov, A. Nassalevska, *J. Power Sources* 43–44 (1993) 561.
- [32] M. Inagaki, K. Otori, T. Tsumura, A. Shimitzu, *Solid State Ionics* 86–88 (1996) 849.
- [33] S. Bach, J.P. Pereira-Ramos, N. Baffier, R. Messina, *J. Electrochem. Soc.* 137 (1990) 1042.
- [34] D.B. Le Passerini, J. Guo, J. Ressler, B.B. Owens, W.H. Smyrl, *J. Electrochem. Soc.* 143 (1996) 2099.
- [35] D. Aurbach, E.M. Shembel, B. Markovsky, R.D. Apostolova, V.M. Nagirny, in preparation.
- [36] H. Kobayashi, *Bull. Chem. Soc. Jpn.* 52 (1979) 1325.
- [37] A. Fotiev, V. Volkov, V. Kapustin, *Oxide Vanadium Bronzes*, Nauka, Moscow, 1978 (in Russian).
- [38] M.G.S.R. Thomas, P.G. Bruce, J.B. Goodenough, *J. Electrochem. Soc.* 132 (1985) 1521.
- [39] W. Weppener, R.A. Huggins, *Annu. Rev. Mater. Sci.* 8 (1978) 269.
- [40] J. Barker, R. Pynenburg, R. Koksang, *J. Power Sources* 52 (1994) 185.
- [41] D. Aurbach, M.D. Levi, E. Levi, B. Markovsky, G. Salitra, H. Teller, U. Heider, V. Hilarius, *Proc. Vol. 97-18, The Electrochem. Soc.*, Pennington, NJ, (1997) 941.
- [42] D. Aurbach, M.D. Levi, B. Markovsky, H. Teller, G. Salitra, *J. Electrochem. Soc.* 145 (1998) 3024.